

RESEARCH ARTICLE

Open Access



RNA sequencing reveals transcriptomic changes in tobacco (*Nicotiana tabacum*) following *NtCPS2* knockdown

Lingxiao He¹, Huabing Liu², Changhe Cheng², Min Xu³, Lei He³, Lihua Li³, Jian Yao³, Wenjun Zhang⁴, Zhengguang Zhai⁴, Qinshan Luo⁵, Jutao Sun¹, Tiezhao Yang¹ and Shixiao Xu^{1*}

Abstract

Background: Amber-like compounds form in tobacco (*Nicotiana tabacum*) during leaf curing and impact aromatic quality. In particular, *cis*-abienol, a polycyclic labdane-related diterpenoid, is of research interest as a precursor of these compounds. Glandular trichome cells specifically express copalyl diphosphate synthase (*NtCPS2*) at high levels in tobacco, which, together with *NtABS*, are major regulators of *cis*-abienol biosynthesis in tobacco.

Results: To identify the genes involved in the biosynthesis of *cis*-abienol in tobacco, we constructed transgenic tobacco lines based on an *NtCPS2* gene-knockdown model using CRISPR/Cas9 genome-editing technology to inhibit *NtCPS2* function in vitro. In mutant plants, *cis*-abienol and labdane diol contents decreased, whereas the gibberellin and abscisic acid (ABA) contents increased compared with those in wild-type tobacco plants. RNA sequencing analysis revealed the presence of 9514 differentially expressed genes (DEGs; 4279 upregulated, 5235 downregulated) when the leaves of wild-type and *NtCPS2*-knockdown tobacco plants were screened. Among these DEGs, the genes encoding *cis*-abienol synthase, ent-kaurene oxidase, auxin/ABA-related proteins, and transcription factors were found to be involved in various biological and physiochemical processes, including diterpenoid biosynthesis, plant hormone signal transduction, and plant-pathogen interactions.

Conclusions: The present study provides insight into the unique transcriptome profile of *NtCPS2* knockdown tobacco, allowing for a better understanding of the biosynthesis of *cis*-abienol in tobacco.

Keywords: CRISPR-Cas9, *Nicotiana tabacum*, RNASeq, Labdanoid diterpenes, *cis*-Abienol, Genome editing, Terpenoids

Background

Aroma is an important attribute of tobacco (*Nicotiana tabacum* L.) leaves. It is an indicator of tobacco quality and is influenced by a variety of chemical components [1]. An important aromatic substance in tobacco leaf surface secretions is *cis*-abienol, which belongs to the

labdanoid diterpenoid family [2, 3]. Previous studies have reported that *cis*-abienol plays an important role in determining the aromatic characteristics of tobacco, and it is an important precursor in the chemical synthesis of amber-like substances [4–6], which can affect aromatic quality. Furthermore, *cis*-abienol is involved in plant resistance to insects [7, 8] and diseases [9]. Therefore, it is important to explore the *cis*-abienol synthesis pathway in tobacco to better understand how to create disease-resistant tobacco varieties with high-quality or characteristic aromas upon flue curing.

* Correspondence: xushixiao@henau.edu.cn

¹College of Tobacco Science, Henan Agricultural University, National Tobacco Cultivation & Physiology & Biochemistry Research Centre, Scientific Observation and Experiment Station of Henan, Ministry of Agriculture, Zhengzhou 450002, China

Full list of author information is available at the end of the article



© The Author(s). 2021 **Open Access** This article is licensed under a Creative Commons Attribution 4.0 International License, which permits use, sharing, adaptation, distribution and reproduction in any medium or format, as long as you give appropriate credit to the original author(s) and the source, provide a link to the Creative Commons licence, and indicate if changes were made. The images or other third party material in this article are included in the article's Creative Commons licence, unless indicated otherwise in a credit line to the material. If material is not included in the article's Creative Commons licence and your intended use is not permitted by statutory regulation or exceeds the permitted use, you will need to obtain permission directly from the copyright holder. To view a copy of this licence, visit <http://creativecommons.org/licenses/by/4.0/>. The Creative Commons Public Domain Dedication waiver (<http://creativecommons.org/publicdomain/zero/1.0/>) applies to the data made available in this article, unless otherwise stated in a credit line to the data.

The biosynthesis of *cis*-abienol in tobacco was initially reported to be controlled by a single gene, *Abl* [10, 11], which is located on chromosome A [12]. Subsequently, Vontimitta et al. [13] used 117 doubled haploid lines and simple sequence repeat molecular markers to locate the genes regulating *cis*-abienol and sucrose ester accumulation and found that both genes are located on chromosome A. The genetic distance between two genes is 8.5 cM, and a total of 17 pairs of markers can be found in the linkage group. Among them, PT10324 and *Abl* are completely separated. The markers beside *Abl* are PT55091 and PT61373, with distances of 2.02 and 0.6 cM, respectively [13]. Copalyl diphosphate synthase 2 (CPS2) from the angiosperm *Cistus creticus subsp. creticus* was first analysed through prokaryotic expression and dephosphorylation. Then, gas chromatography-mass spectrometry (GC-MS) analysis revealed that CPS2 catalyses the formation of 13(E)-labden-8-ol-15-diphosphate, implying that CPS2 is involved in the biosynthesis of *cis*-abienol [14]. In gymnosperms, *cis*-abienol synthase (*ABS/KS*) contains both class I and class II functional domains, as shown by cloning and characterizing the gene from balsam fir (*Abies balsamea*) via transcriptome sequencing [15]. Sallaud et al. [16] cloned *NtCPS2* and *NtABS* from tobacco and showed that both genes are involved in the biosynthesis of *cis*-abienol, which involves two steps. First, CPS-like catalytic activity yields 8-hydroxy-copalyl diphosphate with a normal configuration, which can then be converted to *cis*-abienol by the *NtABS* product [16–18]. No other diterpenoid synthase has been reported to use 8-hydroxy-copalyl diphosphate as a substrate in dicotyledons to date. In addition, promoter analysis of *NtCPS2* showed that it could drive the expression of the *GUS* gene in glandular hairs [16, 19, 20]. The identification of *NtCPS2* and *NtABS* is of great significance for breeding high-quality tobacco and future microbial metabolic engineering. From this knowledge base, other diterpenoid-synthesising genes can be cloned and identified.

Among tobacco types, *cis*-abienol accumulates at different levels. It is mainly found in oriental and cigar tobacco but not in flue-cured tobacco, Burley tobacco, or Maryland tobacco [1, 16, 21]. To study the variation in *cis*-abienol content among different types of cultivated tobacco, 157 varieties of tobacco with or without *cis*-abienol were selected, and the expression levels of *NtCPS2* and *NtABS* were analysed [16]. *NtABS* cDNA sequences did not differ among tobacco varieties, but two distinct polymorphisms were found in *NtCPS2* cDNA: an 8-bp insertion at position 275 and a G-T transversion at position 292 of *NtCPS2*. Both of these result in a stop codon, which leads to early termination and shortening of the encoded peptide chain. Because the encoded protein loses its active site, it also loses its

original function [16]. Thus, *NtCPS2* is key for *cis*-abienol biosynthesis. However, the mechanism by which the metabolic pathway of labdanoid diterpenoids is influenced by *NtCPS2* in tobacco and the effects of *NtCPS2* knockdown on other metabolic pathways are still unknown.

In this study, we used CRISPR/Cas9 gene-editing technology to knock down *NtCPS2*. The CRISPR/Cas9 *NtCPS2* expression vector was constructed from the high-aroma strain 8306 and transformed *NtCPS2*-knockdown plants were obtained. A high-throughput RNA sequencing (RNA-seq) technique was used to compare expression profiles between mutant and 8306 plants. Sequencing results were verified using fluorescence quantitative polymerase chain reaction (PCR), and physiological changes and transcriptional inheritance were analysed. By elucidating the function of the *NtCPS2* gene and the molecular mechanisms underlying the influence of its related genes, high-aroma tobacco varieties can be cultivated.

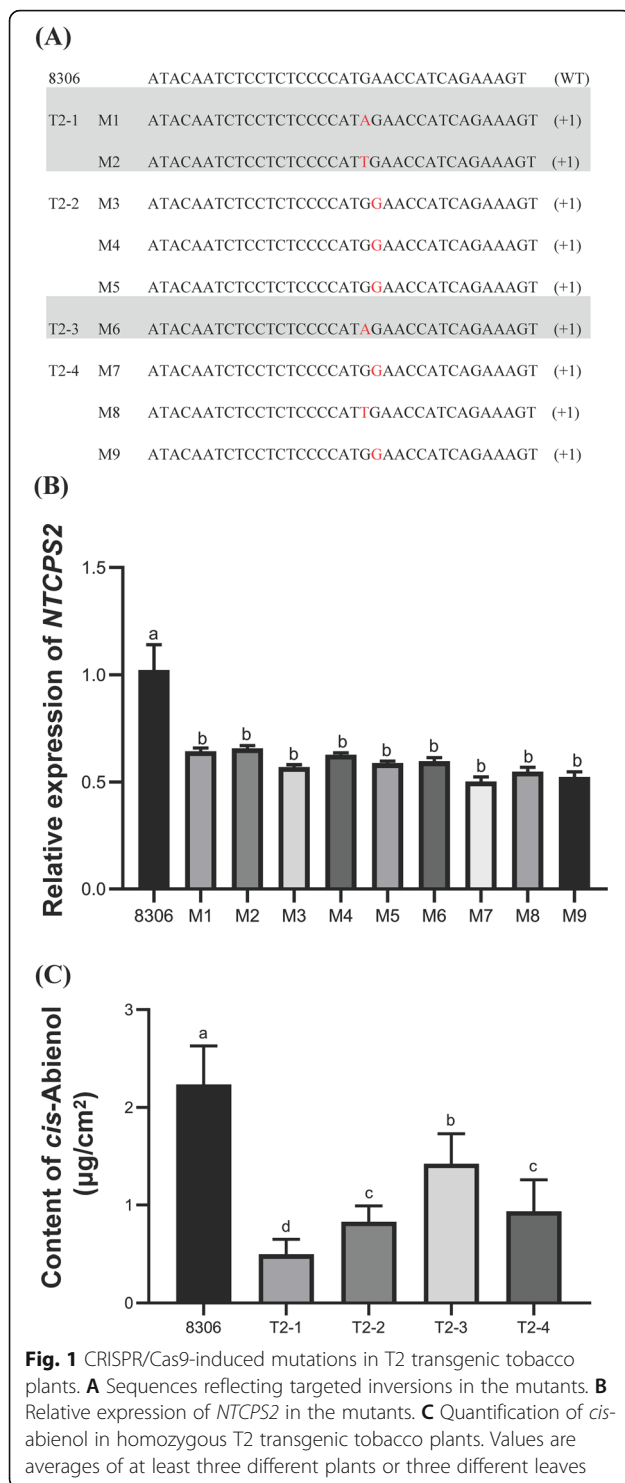
Results

Targeted mutagenesis of *NtCPS2* by CRISPR/Cas9 in tobacco

To generate Cas9-induced mutations in *NtCPS2*, a vector was designed that harboured chimaeric guide RNA (gRNA) to guide Cas9 to target sequences where it bound and cleaved genomic DNA to generate double-strand breaks [22]. Two target sites of *CPS2* were selected (Supplementary Figure 1). The gRNA for each target site was generated by overlap-extension PCR. Cas9 was subcloned into a single expression vector [23]. The Cas9 and gRNA expression cassette was located in one expression vector (pRGEB32-Cas9-NPT II-*CPS2*-gRNA). Through the *Agrobacterium tumefaciens*-mediated method, 36 transformed regenerated plants in the T₀ generation were obtained. After amplification with target-specific primers, all positive samples were sequenced to assess the mutation efficiency. Of 36 plants, eight were transgenic lines. Most of the transgenic lines had a single-base insertion of A, C, or T at Target 2. Thus, as the peptide chain was formed, the stop codon was encountered early in the process, and the translated amino acid chain was greatly shortened. To test the heritability of the mutations, homozygous transgenic plants in the T₀, T₁, and T₂ generations were analysed. Detailed information about the homozygous T₂ plants (M1–M9) is shown in Fig. 1A, and these plants were used for the following experiments.

NtCPS2 knockdown affects *cis*-abienol content

To verify whether the gene mutations caused changes in gene expression, quantitative real-time PCR (qRT-PCR) was used to detect the expression levels of *NtCPS2* in



the leaves of mutant and wild-type (8306) plants. The results showed that *NtCPS2* expression decreased significantly in transgenic plants compared to wild-type plants (Fig. 1B). To detect changes in *cis*-abienol content in the leaves, exudates were collected from the mutant plants and analysed using GC-MS. The contents of *cis*-abienol

also decreased significantly in mutant plants compared to wild-type plants (Fig. 1C). The results indicate that *NtCPS2* is one of the key genes regulating the *cis*-abienol biosynthesis pathway, and *NtCPS2* knockdown results in low levels of *cis*-abienol biosynthesis and accumulation. *NtABS* is another key gene involved in *cis*-abienol biosynthesis [16]. A previous study reported that *cis*-abienol was detected in plants expressing both *NtCPS2* and *NtABS* but not in plants expressing just one of the two genes [16]. *NtABS* expression was weak in the mutant plants compared to the wild-type plants, implying that *NtCPS2* knockdown negatively influenced *NtABS* expression. This is possibly because *NtCPS2* is located upstream of *NtABS* in the *cis*-abienol biosynthesis pathway.

NtCPS2 has a minor effect on the development of glandular trichomes in tobacco

Agronomic characteristics were analysed to assess the mutant phenotypes (Fig. 2 and Supplementary Figure 2). Differences in plant height, internode length, number of leaves, and stem girth between mutant and wild-type plants did not exhibit the same trend. T2–2 mutants had longer internodes and wider stems than other mutants and wild-type plants, whereas all mutants except for T2–1 had shorter plant heights than the wild-type plants (Supplementary Figure 2). These results indicate that *NtCPS2* expression does not strongly affect tobacco plant morphology. As *NtCPS2* is specifically expressed in glandular cells [16], the morphology of the glandular trichomes on the largest leaf of each plant was examined. Both the length and width of the largest leaf were significantly shorter in mutant plants than in wild-type plants. The average diameter of glandular trichomes was smaller in mutant plants, especially T2–1, whereas both longer and shorter glandular trichomes were observed in mutant plants compared to wild-type plants (Fig. 2). Other trichome characteristics, such as the numbers of long and short trichomes, did not differ significantly between mutant and wild-type plants (data not shown). Thus, in the absence of *NtCPS2* expression in tobacco plants, the diameter of glandular cells and the area of the largest leaf decrease, but not the length of glandular trichomes. The T2–1 line was selected and used to profile transcriptomic changes after *NtCPS2* knockdown in tobacco 8306.

Overview of transcriptome sequencing

To profile gene expression after *NtCPS2* knockdown, RNA-seq libraries were constructed for the mutant and wild-type plants. Six samples of each line were sequenced, and 41.64 G of clean data was obtained. In total, 6.70–7.02 G of effective data was collected from each sample, with a Q30 distribution of 94.29–94.91% and an average GC content of 43.41%. More than

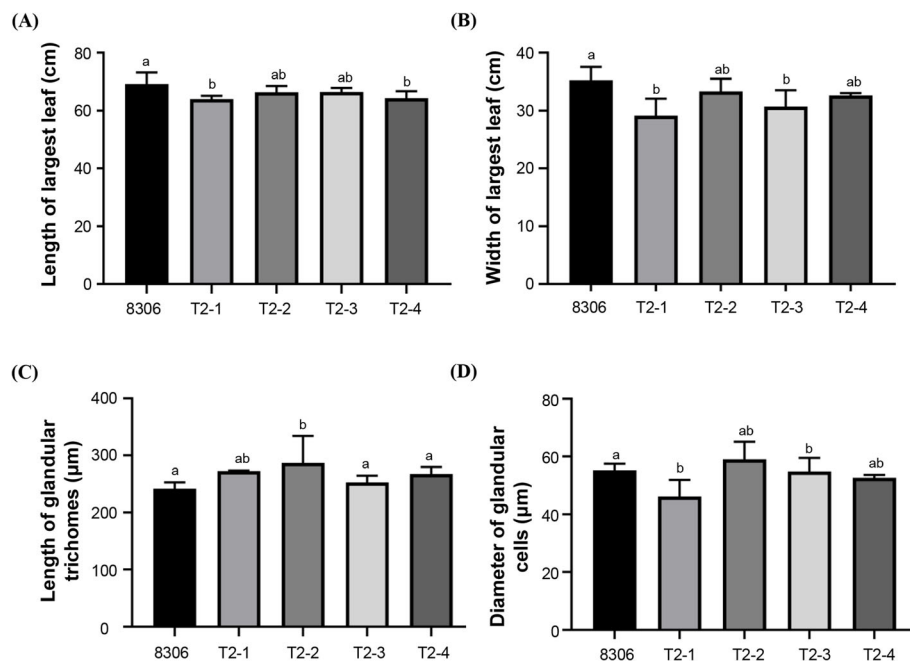


Fig. 2 Morphological characteristics of mutant and wild-type plants, including the length (A) and width (B) of the largest leaf, length of glandular trichomes (C), and diameter of glandular cells (D). Values are presented as the means \pm standard deviations ($n=4$ for leaves and $n=100$ for glandular trichomes). Different lowercase letters denote significant differences among plant lines ($p < 0.05$)

95.58% of the clean reads had quality scores that met the Q30 criterion (probability of base-calling error = 0.1%) [24]. Furthermore, the GC content ranged from 43.15 to 43.66%. The sequencing data are summarized in Table 1.

Analysis of differentially expressed genes (DEGs) and their functions

Volcano plots were used to assess the variation in gene expression between mutant and wild-type plants (Fig. 3A). In total, 9514 DEGs were detected. Among them, 4279 were upregulated and 5235 were downregulated in the transgenic tobacco plants compared to 8103 using the thresholds $p < 0.05$ and $|\log_2(\text{fold change [FC]})| > 1$ (Fig. 3B).

Kyoto Encyclopedia of Genes and Genomes (KEGG) and Gene Ontology (GO) pathway analyses of the differentially expressed mRNAs were performed to determine

the functions of the DEGs. The 20 most significantly enriched pathways (lowest q values) according to KEGG metabolic pathway annotation were examined in detail (Fig. 4A). Based on GO analysis, the DEGs were most likely to be associated with biological processes (Fig. 4B) and cellular components (Fig. 4C). A large percentage of the DEGs were assigned to the categories metabolic process, cellular process, catalytic activity, binding, and single-organism process, with only a few genes assigned to channel regulator activity, cell killing, and protein tag. The DEGs involved in the pathways for diterpenoid biosynthesis, plant hormone signal transduction, and plant-pathogen interactions were analysed in detail.

Validation of selected DEGs using qRT-PCR

To validate the RNA-seq data, 12 DEGs, including genes involved in *cis*-abienol and gibberellin (GA) biosynthesis as well as genes related to plant-pathogen interactions

Table 1 Summary of RNA-sequencing outcomes

Sample	Raw reads	Clean reads	Raw bases	Clean bases	Q30 (%)	GC (%)
Con1	49.05 M	47.90 M	7.36 G	6.89 G	94.60	43.46
Con2	49.76 M	48.74 M	7.46 G	7.02 G	94.88	43.25
Con3	47.66 M	46.51 M	7.15 G	6.70 G	94.29	43.30
L1	49.71 M	48.57 M	7.46 G	6.97 G	94.67	43.66
L2	49.77 M	48.72 M	7.47 G	6.99 G	94.88	43.41
L3	49.70 M	48.62 M	7.45 G	6.97 G	94.85	43.47

Not: Con, wild type; L, mutant

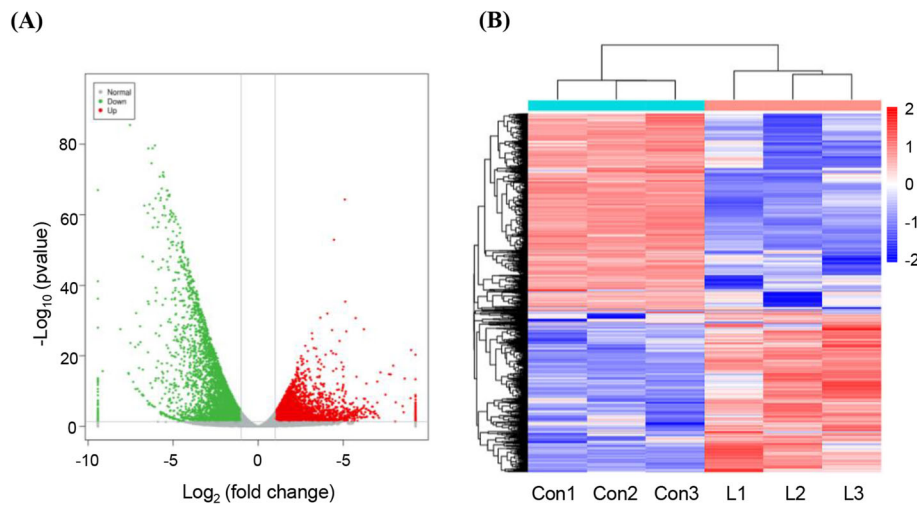


Fig. 3 Differentially expressed genes (DEGs) were screened using an absolute $\log_2(\text{FC})$ value > 1 and p -value < 0.05 . Significant differences in expression were observed for 9514 genes, as represented by a volcano plot (A) and heat map (B)

and other hormone signalling pathways, were selected randomly for qRT-PCR analysis. The gene expression patterns determined using qRT-PCR were consistent with those determined via transcriptome sequencing (Fig. 5). FC values differed between qRT-PCR and RNA-seq, possibly due to differences in the sensitivity of each method or because different samples were used for qRT-PCR and RNA-seq.

Expression levels of genes related to *cis*-abienol biosynthesis decreased significantly in mutant plants

NtCPS2 (Nitab4.5_0001630g0010) was identified as a DEG via RNA-seq, and its expression level was 9.27-fold lower in the mutant than in the wild type. The expression level of another key gene related to *cis*-abienol biosynthesis, *NtABS* (Nitab4.5_0015240g0010), also decreased 2.43-fold in the mutant. *NtCPS2* and *NtABS* operate in succession to synthesize *cis*-abienol [16]. When both *NtCPS2* and *NtABS* are expressed, *cis*-abienol is synthesized and can be detected in plants. However, *cis*-abienol synthesis does not occur in plants that express only one of these genes [16]. *NtCPS2* encodes 8-hydroxy-copalyl diphosphate synthase, which synthesizes 8-hydroxy-copalyl diphosphate, and *NtABS* encodes a kaurene synthase-like (KSL) protein, abienol synthase, which uses 8-hydroxy-copalyl diphosphate to produce *cis*-abienol. Our results indicate that weak expression of *NtCPS2* directly or indirectly results in a decrease in the expression level of *NtABS* and, consequently, low *cis*-abienol contents. Another putative *cis*-abienol synthase (Nitab4.5_0008024g0010) was also found to be downregulated in the mutant, indicating that this enzyme may have the same substrate as *NtABS* and thus be involved in the *cis*-abienol biosynthesis pathway. In contrast,

other putative *cis*-abienol synthases, including Nitab4.5_0004164g0070 and Nitab4.5_0004164g0010, were found to be upregulated in the mutant. These two enzymes may have other functions in tobacco. Other DEGs involved in the *cis*-abienol biosynthesis pathway were also identified (based on KEGG analysis) and had lower expression levels in the mutant (Fig. 4). This included *KSL4* (Nitab4.5_0000029g0200, FC = 2.43) and genes predicted to encode ent-kaur-16-ene synthase (Nitab4.5_0002280g0060, FC = 5.61; and Nitab4.5_0002862g0030, FC = 1.57). As with *KSL4*, *NtABS* is a *KSL* gene (Table 2). Hence, *KSL4* and genes that putatively encode ent-kaur-16-ene synthase may be involved in *cis*-abienol biosynthesis. This needs to be verified in future work.

GA biosynthesis increased significantly in mutant plants

According to diterpenoid biosynthesis pathways, the same substrate, geranylgeranyl pyrophosphate (GGPP), is used for *cis*-abienol and GA synthesis. In this study, most of the DEGs involved in GA biosynthesis were strongly upregulated in the mutant, including *KAO2* (Nitab4.5_0001476g0100, FC = 16.67), *KSI* (Nitab4.5_0004164g0010, FC = 2.76), and *CPS1* (Nitab4.5_0010312g0010, FC = 12.14) (Table 2). From these genes, ent-copalyl diphosphate synthase 1 (encoded by *CPS1*) and ent-kaurene synthase (encoded by *KSI*) were found to separately catalyse the synthesis of ent-kaurene from GGPP. However, *KO* (encodes ent-kaurene oxidase, which converts ent-kaurene to kaur-16-en-18-oate) expression was downregulated in the mutant. DEGs participating in the latter stages of the pathway, such as *KAO2* and *GA20_{OX2}*, were upregulated compared to the wild-type plants. *KO* and *KAO* belong to the CYP701A, P450, and CYP88A clades. Accordingly, *KAO* is localized

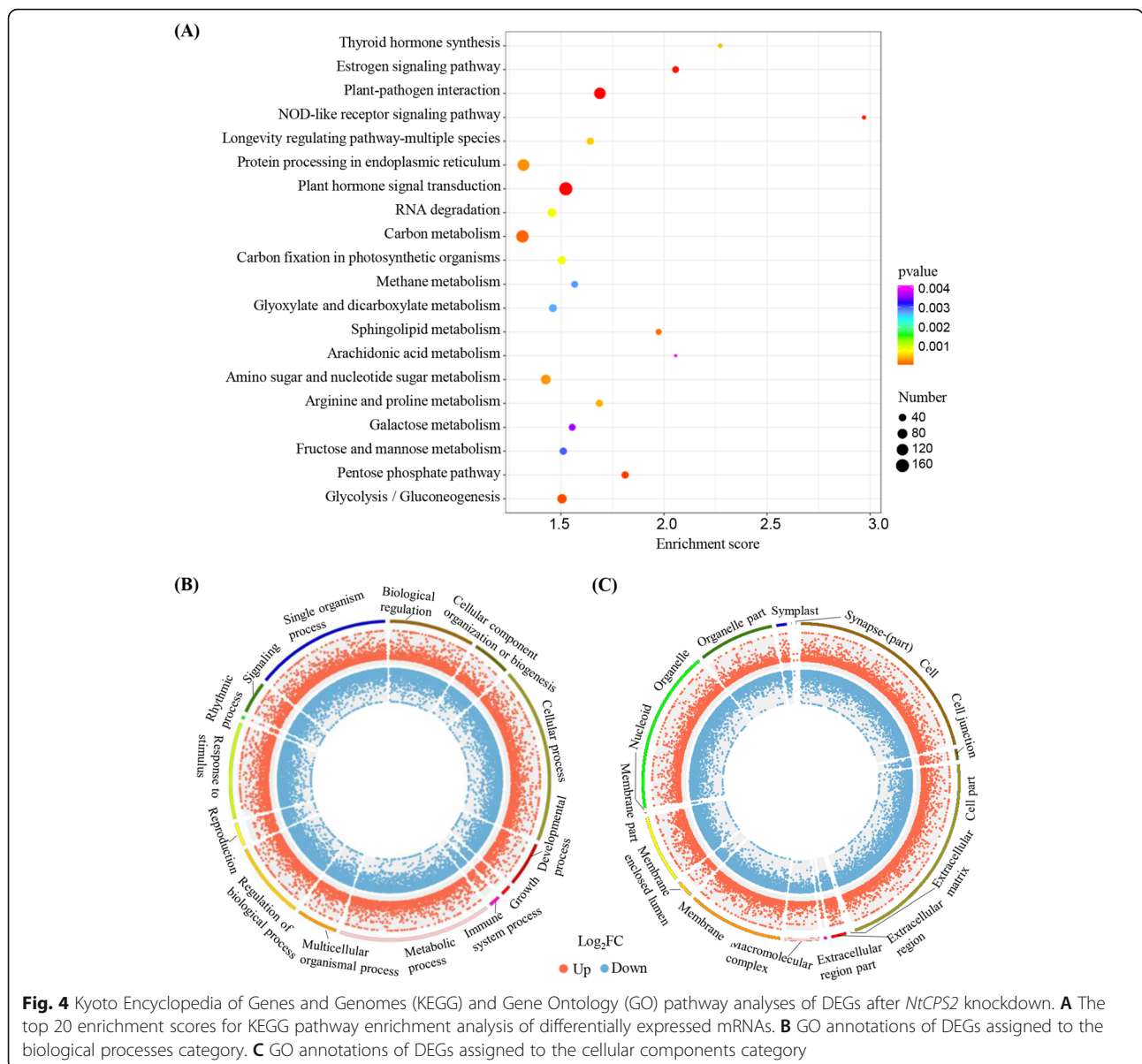


Fig. 4 Kyoto Encyclopedia of Genes and Genomes (KEGG) and Gene Ontology (GO) pathway analyses of DEGs after *NtCPS2* knockdown. **A** The top 20 enrichment scores for KEGG pathway enrichment analysis of differentially expressed mRNAs. **B** GO annotations of DEGs assigned to the biological processes category. **C** GO annotations of DEGs assigned to the cellular components category

in the endoplasmic reticulum, whereas KO is localized in both the endoplasmic reticulum and plastid envelope [25]. The differential expression of *KOI* and *KAO2* in response to *NtCPS2* knockdown was explored further. GA contents in mutant plants were also analysed via GC-MS. The results showed that the GA contents in transgenic plants were significantly higher than those in wild-type plants (Fig. 6). GA12 is considered the precursor of all GAs in plants [26], and other GA forms are produced through oxidative steps catalysed by GA12. Genes involved in the production of these GA forms were up- and downregulated in the mutants.

Changes in abscisic acid (ABA) biosynthesis and signal transduction in mutant plants

In carotenoid biosynthesis pathways, GGPP is also a substrate for ABA synthesis. RNA-seq analysis showed that four *PSY* genes (encoding phytoene synthases) were upregulated at the first step, which involves GGPP, in the mutant compared to the wild type. *PSY* is a transferase enzyme that is involved in the biosynthesis of carotenoids. It catalyses the conversion of GGPP to phytoene. Two genes encoding *LCYs* (lycopene epsilon cyclases) were also upregulated in the mutant at the next step. These results indicate that *NtCPS2* knockdown positively affects ABA synthesis, likely because substrate competition decreases. In addition, two ABA 8'-hydroxylases, which are involved in ABA degradation, were

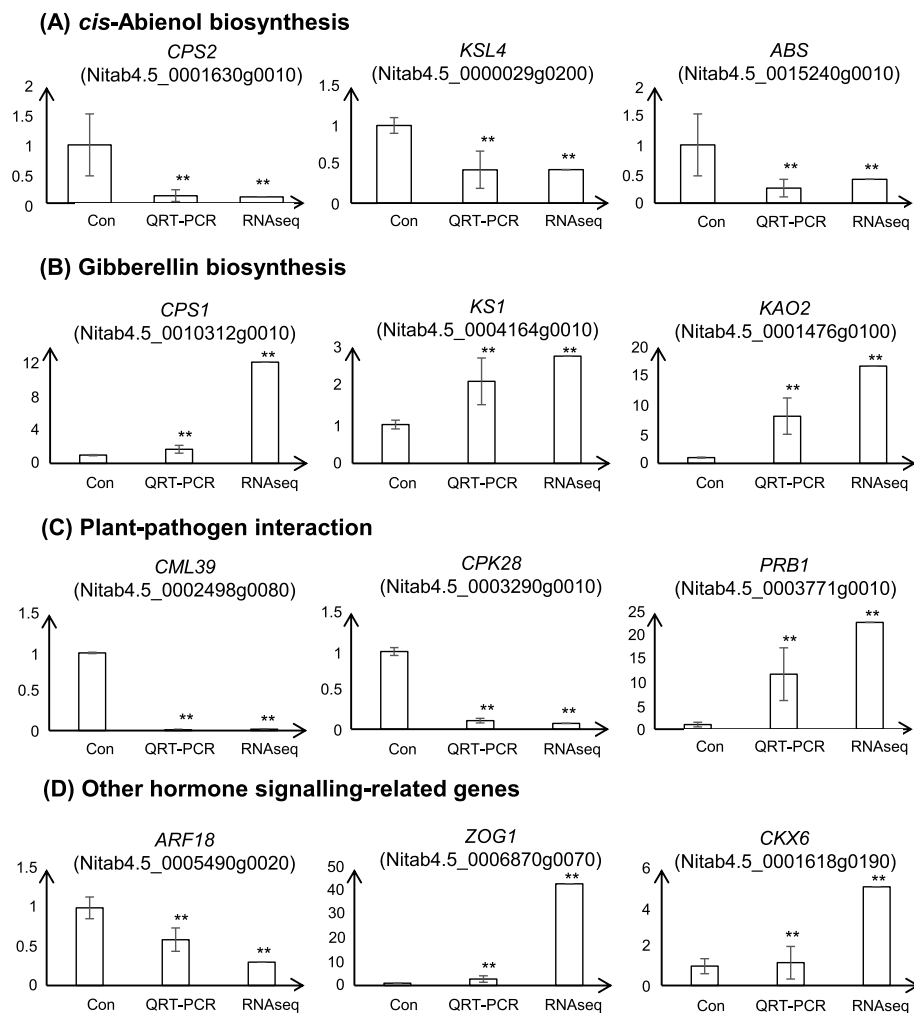


Fig. 5 Transcription profiles of selected genes in mutant and wild-type plants as determined using RNA-seq and quantitative real-time polymerase chain reaction (qRT-PCR). Relative transcription levels of DEGs involved in *cis*-abienol biosynthesis (A), gibberellin (GA) biosynthesis (B), plant-pathogen interactions (C), and other hormone-signalling pathways (D). Asterisks indicate significant differences between samples and the control ($p < 0.05$, two-sample *t*-test)

downregulated in the mutant. In the ABA signal transduction pathway, five of six ABA receptors (PYLs), which inhibit the expression of protein phosphatase 2C, were upregulated in the mutant. In the next step, serine/threonine-protein kinase expression was upregulated in the mutant. This might have been related to stress responses and stomatal opening and closure in tobacco leaves.

Transcriptomic analysis of genes involved in plant-pathogen interactions

In plants, *cis*-abienol may participate in insect resistance and disease resistance [27]. Plant resistance to pathogen attack can induce the accumulation of pathogenesis-related proteins (PRs) that contribute to systematically acquired resistance. In this study, PRs were identified

through RNA-seq. Of the 17 PRs, 14 (82.35%) were significantly upregulated in the mutant compared with the wild type, including genes that encode PR proteins 1A, B, and C (Table 3). Among the 17 families of PRs, PR 1–5, 9–11 and 17 were related to the acquisition of defence against pathogen infections. In addition, calcium is involved in regulating diverse physiological processes as a second messenger [28]. The results of transcriptomic analysis revealed that 15 of 19 CDPKs and most CAM/CML were significantly downregulated upon *NtCPS2* knockdown and a low content of *cis*-abienol, which disturbed the balance among active oxygen species, including rubidium hydroxide, reactive oxygen species, and nitric oxide synthase. Furthermore, the resistance of transgenic tobacco plants to black shank, induced by *Phytophthora nicotianae*, was checked. After the

Table 2 Genes related to diterpenoid biosynthesis that are differentially expressed between *NtCPS2*-knockout and 8306 plants

Gene name	Gene ID	log ₂ FC	Protein properties
<i>CPS2</i>	Nitab4.5_0001630g0010	-3.21	PREDICTED: copal-8-ol diphosphate hydratase, chloroplastic
<i>KSL4</i>	Nitab4.5_0000029g0200	-1.21	PREDICTED: ent-kaur-16-ene synthase, chloroplastic isoform X3
<i>DLO2</i>	Nitab4.5_0000129g0310	-2.53	PREDICTED: gibberellin 2-beta-dioxygenase 8-like
<i>GA2OX2</i>	Nitab4.5_0000222g0140	-5.09	PREDICTED: gibberellin 2-beta-dioxygenase 2
<i>GA2OX1</i>	Nitab4.5_0000923g0050	-3.82	PREDICTED: gibberellin 2-beta-dioxygenase 1-like
<i>GA2OX2</i>	Nitab4.5_0001013g0080	-2.88	PREDICTED: gibberellin 2-beta-dioxygenase 2-like
<i>KAO2</i>	Nitab4.5_0001476g0100	4.06	PREDICTED: ent-kaurenoic acid oxidase 1-like isoform X2
<i>GA20OX2</i>	Nitab4.5_0001573g0060	2.08	gibberellin 20 oxidase 1-like
<i>GA2OX1</i>	Nitab4.5_0002209g0240	-1.46	gibberellin 2-beta-dioxygenase 1-like
<i>KO</i>	Nitab4.5_0002280g0060	-2.49	PREDICTED: ent-kaurene oxidase, chloroplastic
<i>GA2</i>	Nitab4.5_0002862g0030	-1.19	PREDICTED: ent-kaur-16-ene synthase, chloroplastic-like isoform X1
<i>KS1</i>	Nitab4.5_0004164g0010	1.46	PREDICTED: <i>cis</i> -abienol synthase, chloroplastic-like
<i>TPS1</i>	Nitab4.5_0004164g0070	3.00	PREDICTED: <i>cis</i> -abienol synthase, chloroplastic-like
<i>GA2</i>	Nitab4.5_0008024g0010	-1.20	PREDICTED: <i>cis</i> -abienol synthase, chloroplastic-like
<i>CPS1</i>	Nitab4.5_0010312g0010	3.60	PREDICTED: ent-copalyl diphosphate synthase, chloroplastic-like isoform X1
<i>ABS</i>	Nitab4.5_0015240g0010	-1.28	<i>cis</i> -abienol synthase, chloroplastic

FC fold change

treatment of *P. nicotianae* for 7 days, wild-type plants showed wilting symptoms, while the transgenic tobacco plants were not (Supplementary Figure 3).

Discussion

The aromatic characteristics of tobacco are improved by *cis*-abienol, which belongs to the labdane diterpenoid family. Although the genes encoding the enzymes participating in the two steps of *cis*-abienol biosynthesis have been cloned in tobacco [16], the function and transcriptome profile of *NtCPS2* knockdown are less well understood. By knocking down *NtCPS2*, whose product catalyses the first reaction in the *cis*-abienol biosynthesis pathway, we were able to examine how *cis*-abienol

biosynthesis and other related metabolic pathways are controlled. The regulatory network is shown in Fig. 7.

NtCPS2 plays a limited role in the biosynthesis of *cis*-abienol and other terpenoids

Mutations in *NtCPS2* were previously reported to be strongly correlated with the absence of *cis*-abienol and labdane-diol in tobacco or a decrease in their levels [16]. In *N. sylvestris*, *cis*-abienol accumulates when both *NtCPS2* and *NtABS* are expressed [16]. In this study, we generated *NtCPS2*-knockdown tobacco lines using the CRISPR-Cas9 method. In mutant plants that weakly expressed *NtCPS2*, the levels of *cis*-abienol produced decreased (Fig. 1). *NtABS* is involved in the second step of *cis*-abienol biosynthesis, and its expression levels also decreased. The decreased expression of both of these genes might have resulted in low levels of the intermediate 8-hydroxy-copalyl diphosphate accumulating and the cessation of *cis*-abienol production downstream (Fig. 1C). The results indicate that *NtCPS2* plays a key role in *cis*-abienol biosynthesis; thus, downregulated gene expression leads to inactivation of the *cis*-abienol biosynthesis pathway.

The precursor GGPP, which participates in the first step of the pathway, is a common precursor for the biosynthesis of not only diterpenoids (including *cis*-abienol and labdane-diol) but also GA, carotenoids (including ABA), and the phytolchain of chlorophyll [29]. When *NtCPS2* is absent, GGPP is not catalysed to produce 8-hydroxy-copalyl diphosphate, and other reactions that use GGPP as a substrate are enhanced. During GA

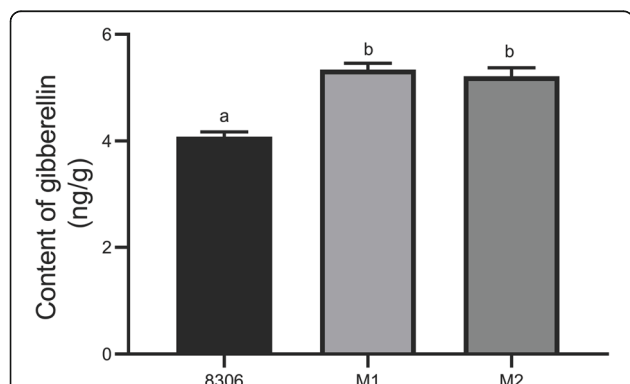


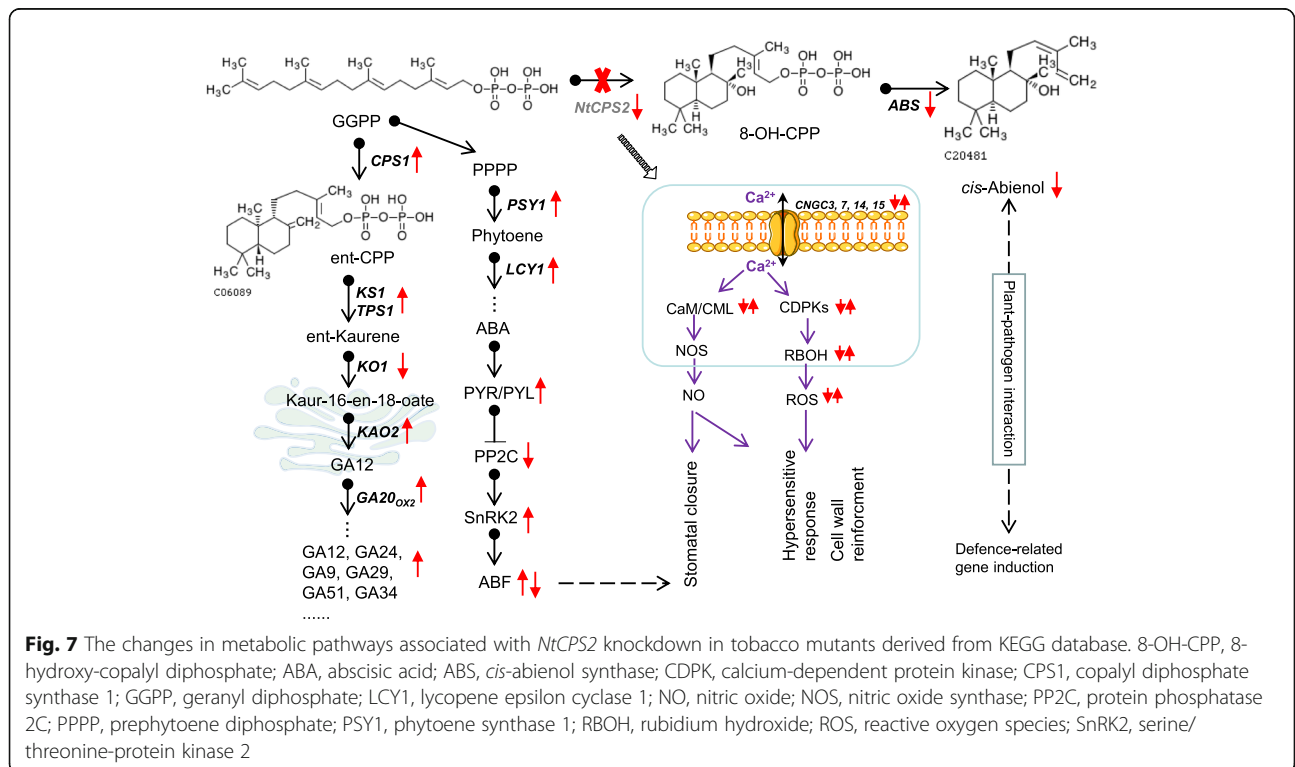
Fig. 6 Gibberellin contents in the leaves of *NtCPS2*-knockdown (M1 and M2) and wild-type (8306) tobacco. Different lowercase letters denote significant differences among plant strains ($p < 0.05$)

Table 3 Properties of DEGs encoding pathogenesis-related proteins

Gene name	Gene ID	log ₂ FC	Protein properties
<i>PRB1</i>	Nitab4.5_0003771g0010	4.52	Pathogenesis-related protein 1A
<i>OSM34</i>	Nitab4.5_0004097g0050	3.76	PREDICTED: pathogenesis-related protein R minor form
<i>PRB1</i>	Nitab4.5_0014031g0010	3.51	PREDICTED: pathogenesis-related protein 1B-like
–	Nitab4.5_0006088g0020	3.46	PREDICTED: pathogenesis-related protein PR-4B
–	Nitab4.5_0018960g0010	3.35	PREDICTED: pathogenesis-related protein PR-4B
–	Nitab4.5_0008835g0020	3.27	PREDICTED: pathogenesis-related protein STH-2-like
–	Nitab4.5_0004861g0030	3.24	PREDICTED: pathogenesis-related protein 1C-like
<i>PRB1</i>	Nitab4.5_0004861g0040	3.16	PREDICTED: pathogenesis-related protein 1C
–	Nitab4.5_0008375g0050	3.06	PREDICTED: pathogenesis-related protein STH-2-like
<i>HEL</i>	Nitab4.5_0009495g0020	2.73	PREDICTED: pathogenesis-related protein PR-4A
<i>TL1</i>	Nitab4.5_0008011g0010	2.29	PREDICTED: pathogenesis-related protein 5-like isoform X1
–	Nitab4.5_0000194g0120	2.17	PREDICTED: pathogenesis-related protein STH-2-like
<i>CRF2</i>	Nitab4.5_0000105g0290	2.06	PREDICTED: pathogenesis-related genes transcriptional activator PTI6-like
<i>CRF2</i>	Nitab4.5_0002902g0060	1.11	PREDICTED: pathogenesis-related genes transcriptional activator PTI6-like
<i>MOS11</i>	Nitab4.5_0002073g0060	–1.47	PREDICTED: pathogenesis-related protein PRMS-like
<i>CRF2</i>	Nitab4.5_0000586g0010	–2.67	PREDICTED: pathogenesis-related genes transcriptional activator PTI6-like
<i>CRF2</i>	Nitab4.5_0007730g0010	–2.72	PREDICTED: pathogenesis-related genes transcriptional activator PTI6-like

biosynthesis in *Arabidopsis*, GGPP is converted to entkaurene in a two-step reaction catalysed by CPS and KS, which are encoded by *AtCPS* and *AtKS*, respectively [30, 31]. In this study, *NtCPS1* and *NtKS1* expression levels were upregulated after *NtCPS2* knockdown, and GA production, which occurs downstream, increased in the

leaves of mutant plants (Fig. 6). In terms of carotenoid biosynthesis, genes (including *phytoene synthase 2* and *lycopene epsilon cyclase*) involved in converting GGPP to phytoene were upregulated after *NtCPS2* knockdown. Overall, reactions that consume GGPP as a substrate were enhanced. The results indicate that *NtCPS2*



knockdown also contributes to the biosynthesis of other terpenoids depending on the same substrate. Future studies can verify this hypothesis by overexpressing *NtCPS2* and/or *NtABS*.

Plants with mutations in *NtCPS2* still exhibit wild-type morphology

Diterpenoids such as cembranoid diterpenes and labdanoid diterpenes from tobacco-leaf exudates significantly influence cigarette smoke characteristics and flavour profiles [2, 3]. To our knowledge, no previous studies on the effects of *cis*-abienol on the growth and development of tobacco plants have been reported. We found that the mutant and wild-type morphology did not differ much, except for the diameter of the glandular trichomes. This indicates that *NtCPS2* knockdown and the subsequent decrease in *cis*-abienol do not affect tobacco plant morphology. However, the contents of other chemical substances (including GA and ABA) may change in mutants. Mutants had higher levels of GA and did not exhibit GA-overdose morphology. In *Arabidopsis*, CPS- and/or KS-overexpressing mutants also did not exhibit GA-overdose morphology [32]. This suggests that the levels of bioactive GA in these plants likely did not change. Transcriptomic analysis showed that the expression of $GA20_{OX2}$ was upregulated, whereas that of $GA2_{OX4}$, $GA2_{OX2}$, and $GA2_{OX1}$ was downregulated (Table 2). Wild-type *Arabidopsis* plants treated with exogenous GA and transgenic plants overexpressing the downstream GA biosynthesis gene *AtGA20_{ox1}* both exhibited aspects of GA overdose morphology [33]. The differential regulation of $GA20_{OX}$, $GA2_{OX4}$, $GA2_{OX2}$, and $GA2_{OX1}$ might result in different types of GA accumulating at different levels; thus, overall levels of bioactive GA may not change much, and plants may not exhibit a GA-underdose morphology.

cis-abienol may participate in tobacco disease resistance

Labdanoid diterpenes may exhibit defence-related activities such as antifungal [9] and insecticidal [7, 8] activities [27, 34]. The application of *cis*-abienol to the roots of tobacco, tomato, and *Arabidopsis* at a concentration of 100 $\mu\text{mol/L}$ can induce the expression of resistance genes and inhibit bacterial wilt disease [27]. In vitro experiments showed that concentrations of *cis*-abienol and related diterpenoids in the range of 0.01–100 ppm can inhibit the growth of *Phytophthora nicotianae* in tobacco [35]. However, *cis*-abienol isolated from *Cunninghamia konishii* had no inhibitory effect on the growth of wood decay fungi [36]. Kennedy et al. [37] found that the concentration of *cis*-abienol from $3.75 \times 10^{-4} \mu\text{g/cm}^2$ to $120 \mu\text{g/cm}^2$ had inhibitory effect on *Peronospora tabacina*. Compared with the control, the germination of sporangia was not affected by 10 kinds of *cis*-abienol

concentrations. At the two lowest concentrations, $3.75 \times 10^{-4} \mu\text{g/cm}^2$ and $3.75 \times 10^{-3} \mu\text{g/cm}^2$, the incidence rate of *Peronospora tabacina* in tobacco was higher than that in the control group. In this study, the resistance of *NtCPS2* mutant tobacco lines to black shank was better than that of wild-type plants. Under field conditions, *cis*-abienol does not have an effect on diseased leaves in tobacco. QTL Phn15.1 in the cigar tobacco cultivar Beinhart 1000 was discovered, which provides a high level of partial resistance to black shank disease caused by *P. nicotianae* [13, 38]. A very close genetic association was found between Phn15.1 and the ability to biosynthesize *cis*-abienol. Recently, Steede et al. [35] observed no correlation between field resistance to *P. nicotianae* and the ability to accumulate *cis*-abienol in either transgenic materials or mapping populations. *Cis*-Abienol has little effect on black shank disease development under natural field conditions. Therefore, whether the accumulation of *cis*-abienol and the genes related to *cis*-abienol synthesis contributed to resistance against *P. nicotianae* in tobacco needs to be explored further. In this study, *NTCP S2* was edited to construct transgenic materials with low *cis*-abienol content. It was found that the transgenic materials were sick later than the wild-type in response to *Phytophthora nicotianae* treatment. In the subsequent experiments, we found that the ratio of GA_3/ABA changed, which may have an impact on the resistance of transgenic materials.

A key defence response to pathogen attack in plants is the induction and accumulation of various PR proteins, which also contribute to systematically acquired resistance [39, 40]. The PR-1, PR-2 [41], PR-3, PR-4, PR-5 [42], PR-9 [43], PR-10 [44], PR-11 [45], and PR-17 [46] families are associated with acquired resistance to pathogen infections. Among the genes encoding these PR proteins, *PR-1* is generally considered a marker gene for disease resistance [47]. In this study, PR-related genes were both significantly up- and downregulated in the mutant plants (Table 3), implying that *cis*-abienol may participate in *Tobacco curly shoot virus* resistance in tobacco plants. Future research could assess disease resistance in *NtCPS2*-knockdown and *NtCPS2*-overexpressing mutants to clarify the contribution of *cis*-abienol to tobacco disease resistance.

Conclusions

In this study, a genome-wide transcription profile was obtained for *NtCPS2*-knockdown tobacco plants edited using CRISPR-Cas9. *NtCPS2* is a key gene for *cis*-abienol biosynthesis in tobacco. Genes involved in the biosynthesis of *cis*-abienol, early metabolites of GA, and carotenoids (including ABA) were significantly differentially expressed after *NtCPS2* knockdown. The expression of PR-related genes also changed in response to low *cis*-

abienol contents. Our findings may be useful for further investigation of the molecular mechanisms associated with *NtCPS2* gene function and the synthesis of *cis*-abienol. Additionally, our results can contribute to the development of high-aroma tobacco varieties.

Methods

Tobacco plant culture and inoculation

The tobacco plant variety (*N. tabacum* cv. 8306) used in this study produces high-aroma, flue-cured tobacco with high levels of *cis*-abienol. Plants were grown in scientific and educational park with loamy tidal soil of Henan Agricultural University, Zhengzhou City, China (113.63E, 37.75 N). Wild-type and transgenic tobacco plants were cultured and grown in mixed soil (1:1 vermiculite:humus) in a growth chamber at 22 °C with 250–300 $\mu\text{mol}/\text{m}^2/\text{s}$ photosynthetically available radiation and a 16-h light/8-h dark cycle. Measurements of leaf age started when the length of the middle leaf of each plant reached 1.5 cm. At a leaf age of 60 days, five tobacco plants at the same developmental stage from each group were selected, and the middle leaves were sampled for the measurements of morphological characteristics and RNA extraction. Seeds were collected at 25 days after flowering. *Phytophthora nicotianae* was cultivated at 24 °C on clarified V8-Agar, and Zoospores were produced under aseptic conditions [48]. The treatment was applied at the stage around third leaf stage of wild-type and transgenic tobacco plants. Small areas of source leaves were infiltrated with a suspension containing 600–900 zoospores μL for 7 days [49]. Control tissues were infiltrated with sterile tap water.

Vector construction

Based on the mRNA sequences and corresponding genome sequences, two CRISPR target sites (Supplementary Table 1) were designed to improve gene-targeting efficiency. Target primers for PCR (Supplementary Table 2) were designed and synthesized. After primer synthesis, fragments containing the target sites were amplified using overlap-extension PCR. The amplified fragments were cloned into a CRISPR expression vector using a recombinant enzyme from Nanjing Novozan Biotechnology Co., Ltd. (Nanjing, China). The CRISPR vector was electroporated into *Escherichia coli*, and positive clones were screened using colony PCR for *Agrobacterium tumefaciens*-mediated transformation and tobacco gene transformation.

Agrobacterium-mediated transformation

Agrobacterium tumefaciens-mediated transformation was performed as follows: 5 μL of recombinant plasmid was mixed with 50 μL of competent *Agrobacterium tumefaciens* cells on ice for 30 min. Blank YEB medium

was added, and the mixture was incubated at 28 °C for 12–13 h. Then, the mixture was transferred to YEB solid medium containing 50 mg/L kanamycin and incubated at 28 °C for 36–48 h. Mature tobacco seeds were sterilized by washing with 75% alcohol and 10% sodium hypochlorite and placed into germination medium. The seeds were then grown under light for 45 days. Samples with a diameter of 0.5 cm were taken from leaves with a hole punch, transferred to a preculture medium, and incubated for 2 days under light. *Agrobacterium tumefaciens* was activated in medium containing 50 mg/L kanamycin. Leaf discs were infected with *Agrobacterium tumefaciens*, transferred to coculture medium, and left for 3 days. Thereafter, the leaf discs were washed with sterilized distilled water and antibiotics in an aqueous solution. After the leaves were dried, they were transferred to a screening medium and cultured under light. After differentiation, they were transferred to rooting medium. Transformed plants were obtained by rooting culture and transplanted into soil after 1 month.

DNA extraction and sequencing for detecting mutations in the target gene

Leaflets were collected from each plant, and genomic DNA was extracted using a standard cetrimonium bromide protocol. NPTII-specific primers were used to detect successfully transformed plants via PCR (Supplementary Table 3). After confirming that the exogenous DNA fragment had been inserted, the primer 17KN48 was designed based on the *NtCPS2* gene sequence and target-site location to detect positive plants using PCR. PCR amplification was performed in the following reaction volume: 1 μL of DNA, 2 μL of 10 \times PCR buffer, 0.4 μL of dNTP mixture, 0.2 μL of forward and reverse primers, 0.2 μL of rTaq DNA polymerase (TOYOBO, Osaka, Japan), and 20 μL of diethyl pyrocarbonate-treated water. PCR was carried out using the following programme: 94 °C for 3 min, 94 °C for 30 s, 55 °C for 30 s, 72 °C for 30 s, 72 °C for 10 min, and 25 °C for 1 min for 30 cycles. The PCR products were detected using gel electrophoresis and sequenced.

Measurements of morphological characteristics of transgenic tobacco plants

Homozygous T₂ tobacco plants were selected, and morphological parameters, including plant height, number of leaves, stem girth, internode length, and length and width of the largest leaf, were measured at a leaf age of 60 days. The morphology of leaf glandular trichomes was also characterized. The largest leaves of each plant of the same age were detached, and the epidermis at the centre of each leaf was peeled off to examine the glandular trichomes using an Axioplan 2 microscope (Carl Zeiss, Oberkochen, Germany). The numbers of long and

short glandular trichomes were counted, and their lengths and diameters were measured. Each seedling had an average of approximately 100 glandular trichomes.

Analysis of diterpenoids in leaf exudates using GC-MS

Leaf exudates were sampled from fresh tobacco leaves, and 1:1 portions of the samples were directly injected into a 6890 N gas chromatograph coupled to a 5973 N mass spectrometer (Agilent Technologies, Santa Clara, CA, USA) for GC-MS analysis. Tobacco diterpenoids were identified based on their mass spectra.

RNA-seq analysis

The middle leaves of wild-type and transgenic tobacco were sampled at a leaf age of 60 days. Total RNA was extracted from frozen leaf samples using TRIzol reagent (Invitrogen, Carlsbad, CA, USA) according to the manufacturer's protocol. RNA integrity was assessed using agarose gel electrophoresis, and RNA purity was checked using a NanoPhotometer® spectrophotometer (Implen, Munich, Germany). RNA concentration was quantified with a Qubit®2.0 Fluorometer using a Qubit® RNA Assay kit (Life Technologies, Carlsbad, CA, USA). From each qualified sample, 3 µg of RNA was sent to Illumina (San Diego, CA, USA) for sequencing. The cDNA library was prepared for sequencing according to the Illumina TruSeq™ RNA Sample Kit protocol. Sequencing was performed using an Illumina HiSeq 2500 system. RNA-seq reads were generated and processed to calculate expression levels, which were averaged over three biological replicates.

Bioinformatics analysis of RNA-seq data

Raw reads were processed through in-house Perl scripts. Clean reads were obtained by removing adapter-containing reads, reads containing poly-N, and low-quality reads from the raw reads. The clean reads were then mapped to the tobacco reference genome (ftp://anonymous@ftp.solgenomics.net/genomes/Nicotiana_tabacum/assembly/K326). Using Hisat2 v2.0.5 (ftp://ftp.ensembl.org/pub/release-94/gtf/mus_musculus/), an index of the reference genome was built, and paired-end clean reads were aligned to the reference genome. We selected Hisat2 as the mapping tool because it can generate a database of splice junctions based on the gene model annotation file and thus produce better mapping results than other nonsplice mapping tools. The expression level of each gene was normalized to fragments per kilobase per million for comparison among different samples. Differential expression analysis was performed using the DESeq2 R package (1.16.1) [50], and an absolute $\log_2(\text{FC})$ value > 1 and a corrected p -value < 0.05 were set as the thresholds for DEGs for subsequent analysis.

DEGs were further annotated using GO functional enrichment analysis. GO terms with corrected p -values < 0.05 were considered to be significantly enriched for a given DEG. Clusters of orthologous groups and pathway analyses were performed using KEGG (<http://www.genome.jp/kegg>) analytical tools. We used the clusterProfiler R package [51] to test the statistical enrichment of KEGG pathways for the DEGs.

Validation of DEGs using qRT-PCR

The differential expression of 20 genes between wild-type and transgenic tobacco leaf samples was confirmed using qRT-PCR analysis with three biological replicates per sample. Primer sets for the DEGs were designed using Primer Premier 5.0 (Premier Biosoft, San Francisco, CA, USA) and synthesised by Invitrogen Trading (Shanghai) Co., Ltd. (China). All primer sequences are listed in Supplementary Table 4. RNA isolation, cDNA synthesis, qRT-PCR, and statistical analyses were performed as previously described [52]. The expression levels of the DEGs were normalized to that of the internal control gene L25 [53].

Statistical analyses

Data are presented as the means ± standard deviations. Two-sample t-tests were used to compare the means between two treatments. Comparisons across multiple treatments were performed using one-way analysis of variance followed by Tukey's honestly significant difference post hoc test with SPSS v19 software (IBM Corporation, Armonk, NY, USA). A value of $p < 0.05$ was taken to denote statistical significance.

Abbreviations

CPS: Copalyl diphosphate synthase; ABA: Abscisic acid; GC-MS: Gas chromatography-mass spectrometry; ABS: Abienol synthase; RNA-seq: RNA sequencing; qRT-PCR: Quantitative real-time polymerase chain reaction; KSL: Kaurene synthase-like; KO: ent-kaurene oxidase; DEGs: Differentially expressed genes; KEGG: Kyoto encyclopedia of genes and genomes; GO: Gene ontology; PSY: Phytoene synthases; LCYs: Lycopene epsilon cyclases; PRs: Pathogenesis-related proteins

Supplementary Information

The online version contains supplementary material available at <https://doi.org/10.1186/s12864-021-07796-8>.

Additional file 1: Table S1. The sequences of target sites.

Additional file 2: Table S2. The primers for PCR amplification.

Additional file 3: Table S3. NPTII specific primers and 17KN48 target primers.

Additional file 4: Table S4. Primer sequences for qRT-PCR.

Additional file 5: Figure S1. The target sites of *NtCPS2*.

Additional file 6: Figure S2. Morphological characteristics of mutant and wild-type plants, including plant height (A), internode length (B), number of leaves (C) and girth of stem (D). Values are presented as the means ± standard deviations ($n = 4$ for leaves and $n = 100$ for glandular

trichomes). Different lowercase letters denote significant differences among plant lines ($p < 0.05$).

Additional file 7: Figure S3. Seedlings of wild-type and transgenic tobacco plants before (A) and after treatment of *Phytophthora nicotianae* infection for 7 days (B).

Acknowledgments

We thank Yongle Ding, Zhaoyun Wu, Dongfang Cai, Gang Xue and Qingquan Xu for their help.

Authors' contributions

Conceptualization, S.X., and T.Y.; methodology, C.C. and L.H.1; software, L.H.2; validation, T.Y.; formal analysis, J.S. and S.X.; investigation, H.L. and T.Y.; data curation, J.S. and S.X.; writing—original draft preparation, S.X.; writing—review and editing, S.X. and T.Y.; funding acquisition, T. Y, S.X., and L.H.1. Revising the manuscript: M.X., L.H.1, L.L., J.Y., W.Z., Z.Z., Q. L and S.X. All authors have read and agreed to the published version of the manuscript.

Funding

This research was funded by China National Tobacco Corporation Henan company ([2021]27), Henan Tobacco Corporation XuChang Company (2020411000240069), Guizhou Tobacco Corporation Guiyang company (2020–07), Hunan Tobacco Corporation Changsha Company (21–23A04), Guangxi Zhuang Autonomous Region Tobacco Corporation Baise Company(2021–4).

Availability of data and materials

The online version contains supplementary material available at <https://www.ncbi.nlm.nih.gov/bioproject/?term=prjna734477>, numbered PRJNA734477 in *Nicotiana tabacum* Raw sequence reads (TaxID: 4097).

Declarations

Ethics approval and consent to participate

Not applicable.

Consent for publication

Not applicable.

Competing interests

The authors declare no conflict of interest.

Author details

¹College of Tobacco Science, Henan Agricultural University, National Tobacco Cultivation & Physiology & Biochemistry Research Centre, Scientific Observation and Experiment Station of Henan, Ministry of Agriculture, Zhengzhou 450002, China. ²Technology Center, China Tobacco Zhejiang Industry Co, Ltd., Hangzhou 310008, China. ³China National Tobacco Corporation Henan company, Zhengzhou 450002, Henan, China. ⁴Hunan Tobacco Corporation Changsha Company, Changsha 410007, Hunan, China. ⁵Guangxi Zhuang Autonomous Region Tobacco Corporation Baise Company, Baise 533000, Guangxi, China.

Received: 26 September 2020 Accepted: 10 June 2021

Published online: 23 June 2021

References

- Popova V, Ivanova T, Prokopov T, Nikolova M, Stoyanova A, Zheljzakov VD. Carotenoid-related volatile compounds of tobacco (*Nicotiana tabacum* L.) essential oils. *Molecules*. 2019;24(19):3446.
- Wagner GJ. Elucidation of the functions of genes central to diterpene metabolism in tobacco trichomes using posttranscriptional gene silencing. *Planta*. 2003;216(4):686–91.
- Yan N, Du Y, Liu X, Zhang HB, Liu YH, Zhang P, et al. Chemical structures, biosynthesis, bioactivities, biocatalysis and semisynthesis of tobacco cembranoids: An overview. *Ind Crop Prod*. 2016;83:66–80. <https://doi.org/10.1016/j.indcrop.2015.12.031>.
- Koyama H, Kaku Y, Ohno M. Synthesis of ambrox from L-abiatic acid. *Tetrahedron Lett*. 1987;28(25):2863–6. [https://doi.org/10.1016/S0040-4039\(00\)96229-4](https://doi.org/10.1016/S0040-4039(00)96229-4).
- Barrero AF, Alvarez-Manzaneda EJ, Altarejos J, Salido S, Ramos JM. Synthesis of ambrox(R) from (–)-sclareol and (+)-cis-abienol. *Tetrahedron*. 1993;49(45):10405–12. [https://doi.org/10.1016/S0040-4020\(01\)80567-6](https://doi.org/10.1016/S0040-4020(01)80567-6).
- Bolster MG, Jansen BJM, Groot A. The synthesis of (–)-Ambrox((R)) starting from labdanolic acid. *Tetrahedron*. 2001;57(26):5657–62. [https://doi.org/10.1016/S0040-4020\(01\)00493-8](https://doi.org/10.1016/S0040-4020(01)00493-8).
- Lin Y, Wagner GJ. Surface disposition and stability of pest-interactive, Trichome-exuded diterpenes and sucrose esters of tobacco. *J Chem Ecol*. 1994;20(8):1907–21. <https://doi.org/10.1007/BF02066232>.
- Kennedy BS, Nielsen MT, Severson RF. Biorationals from nicotiana protect cucumbers against colletotrichum-lagenarium (pass) ell and halst-disease development. *J Chem Ecol*. 1995;21(2):221–31. <https://doi.org/10.1007/BF02036653>.
- Kennedy BS, Nielsen MT, Severson RF, Sisson VA, Stephenson MK, Jackson DM. Leaf surface chemicals from Nicotiana affecting germination of Peronospora-Tabacina (Adam) sporangia. *J Chem Ecol*. 1992;18(9):1467–79. <https://doi.org/10.1007/BF00993221>.
- Tomita H, Sato M, Kawashima N. Inheritance of labdanoid producing ability in *Nicotiana tabacum*. *Agric Biol Chem*. 1980;44:2517–8.
- Wagner G. Leaf surface chemistry. In: *Tobacco Production, Chemistry and Technology*. Blackwell Science; 1999. p. 292–303.
- Kubo T, Sato M, Tomita H, Kawashima N. Identification of the chromosome carrying the gene for cis-abienol production by the use of monosomics in *Nicotiana tabacum* L. *Tob Int*. 1982;184(23):57–9.
- Vontimitta V, Danehower DA, Steede T, Moon HS, Lewis RS. Analysis of a *Nicotiana tabacum* L.genomic region controlling two leaf surface chemistry traits. *J Agric Food Chem*. 2010;58(1):294–300. <https://doi.org/10.1021/jf903256h>.
- Farala V, Pichersky E, Kanellis AK. A Copal-8-ol diphosphate synthase from the angiosperm *cistus creticus* subsp *creticus* is a putative key enzyme for the formation of pharmacologically active, oxygen-containing labdane-type diterpenes. *Plant Physiol*. 2010;154(1):301–10. <https://doi.org/10.1104/pp.110.159566>.
- Zerbe P, Chiang A, Yuen M, Hamberger B, Hamberger B, Draper JA, et al. Bifunctional cis-abienol synthase from *Abies balsamea* discovered by transcriptome sequencing and its implications for diterpenoid fragrance production. *J Biol Chem*. 2012;287(15):12121–31. <https://doi.org/10.1074/jbc.M111.317669>.
- Sallaud C, Giacalone C, Töpfer R, Goepfert S, Bakaher N, Rösti S, et al. Characterization of two genes for the biosynthesis of the labdane diterpene Z-abienol in tobacco (*Nicotiana tabacum*) glandular trichomes. *Plant J*. 2012;72(1):1–17. <https://doi.org/10.1111/j.1365-313X.2012.05068.x>.
- Carman RM, Duffield AR. The biosynthesis of labdanoids – the optical purity of naturally-occurring manool and abienol. *Aust J Chem*. 1993;46(7):1105–14. <https://doi.org/10.1071/CH9931105>.
- Guo ZH, Wagner GJ. Biosynthesis of labdenediol and sclareol in cell-free extracts from trichomes of *Nicotiana glutinosa*. *Planta*. 1995;197(4):627–32.
- Cui H, Zhang ST, Yang HJ, Ji H, Wang XJ. Gene expression profile analysis of tobacco leaf trichomes. *BMC Plant Biol*. 2011;11(1):76. <https://doi.org/10.1186/1471-2229-11-76>.
- Wang EM, Gan SS, Wagner GJ. Isolation and characterization of the CYP71D16 trichome-specific promoter from *Nicotiana tabacum* L. *J Exp Bot*. 2002;53(376):1891–7. <https://doi.org/10.1093/jxb/erf054>.
- Severson RF, Arrendale RF, Chortyk OT, Johnson AW, Gwynn GR, Chaplin JF, et al. Quantitation of the major cuticular components from green leaf of different tobacco types. *J Agric Food Chem*. 1984;32(3):1023–30.
- Jinek M, Chylinski K, Fonfara I, Hauer M, Doudna JA, Charpentier E. A programmable dual-RNA-guided DNA endonuclease in adaptive bacterial immunity. *Science*. 2012;337(6096):816–21. <https://doi.org/10.1126/science.1225829>.
- Li JF, Norville JE, Aach J, McCormack M, Zhang D, Bush J, et al. Multiplex and homologous recombination-mediated genome editing in *Arabidopsis* and *Nicotiana benthamiana* using guide RNA and Cas9. *Nat Biotechnol*. 2013;31(8):688–91. <https://doi.org/10.1038/nbt.2654>.
- Peng D, Tarleton R. EuPaGDT: a web tool tailored to design CRISPR guide RNAs for eukaryotic pathogens. *Microb Genom*. 2015;1(4):e000033.
- Helliwell CA, Sullivan JA, Mould RM, Gray JC, Peacock WJ, Dennis ES. A plastid envelope location of *Arabidopsis* ent-kaurene oxidase links the plastid and endoplasmic reticulum steps of the gibberellin biosynthesis pathway. *Plant J*. 2001;28(2):201–8. <https://doi.org/10.1046/j.1365-313X.2001.01150.x>.

26. Hedden P, Phillips AL. Gibberellin metabolism: new insights revealed by the genes. *Trends Plant Sci.* 2000;5(12):523–30. [https://doi.org/10.1016/S1360-1385\(00\)01790-8](https://doi.org/10.1016/S1360-1385(00)01790-8).
27. Seo S, Gomi K, Kaku H, Ab H, Seto H, Nakatsu S, et al. Identification of natural diterpenes that inhibit bacterial wilt disease in tobacco, tomato and Arabidopsis. *Plant Cell Physiol.* 2012;53(8):1432–44. <https://doi.org/10.1093/pcp/pcs085>.
28. Poovaih BW, Reddy ASN. Calcium and signal transduction in plants. *Crit Rev Plant Sci.* 1993;12(3):185–211. <https://doi.org/10.1080/07352689309701901>.
29. Takahashi N, Phinney BO, MacMillan J, editors. *Gibberellins*. New York: Springer-Verlag; 1991. <https://doi.org/10.1007/978-1-4612-3002-1>.
30. Yamaguchi S. Gibberellin metabolism and its regulation. *Annu Rev Plant Biol.* 2008;59(1):225–51. <https://doi.org/10.1146/annurev.arplant.59.032607.092804>.
31. Yamaguchi S, Sun TP, Kawaide H, Kamiya Y. The GA2 locus of *Arabidopsis thaliana* encodes ent-kaurene synthase of gibberellin biosynthesis. *Plant Physiol.* 1998;116(4):1271–8. <https://doi.org/10.1104/pp.116.4.1271>.
32. Fleet CM, Yamaguchi S, Hanada A, Kawaide H, David CJ, Kamiya Y, et al. Overexpression of *AtCPS* and *AtKS* in *Arabidopsis* confers increased ent-kaurene production but no increase in bioactive gibberellins. *Plant Physiol.* 2003;132(2):830–9. <https://doi.org/10.1104/pp.103.021725>.
33. Hedden P, Phillips AL, Rojas MC, Carrera E, Tudzynski B. Gibberellin biosynthesis in plants and fungi: a case of convergent evolution? *J Plant Growth Regul.* 2002;20:319–31.
34. Severson R, Johnson A, Jackson D. Cuticular constituents of tobacco: factors affecting their production and their role in insect and disease resistance and smoke quality. *Recent Adv Tobacco Sci.* 1985;11:105–74.
35. Steede WT, Ma JM, Eickholt DP, Drake-Stowe KE, Kernodle SP, Shew HD, et al. The tobacco trichome exudate z-abienol and its relationship with plant resistance to *Phytophthora nicotianae*. *Plant Dis.* 2017;101(7):1214–21. <https://doi.org/10.1094/PDIS-10-16-1512-RE>.
36. Cheng SS, Chung MJ, Lin CY, Wang YN, Chang ST. Phytochemicals from *Cunninghamia konishii* Hayata act as antifungal agents. *J Agric Food Chem.* 2012;60(1):124–8. <https://doi.org/10.1021/jf2042196>.
37. Kenedy BS, Nnensen MT, Severson RF, et al. Leaf surface chemicals from *Nicotiana* affecting germination of *Peronospora tabacina* (adam) sporangia. *J Chem Ecol.* 1992;18(9):1467–78. <https://doi.org/10.1007/BF00993221>.
38. Vontimitta V, Lewis RS. Growth chamber evaluation of a tobacco 'Beinhart 1000' × 'Hicks' mapping population for quantitative trait loci affecting resistance to multiple races of *Phytophthora nicotianae*. *Crop Breed Genet.* 2012;52:91–8.
39. Van LL, Rep M, Pieterse CM. Significance of inducible defense-related proteins in infected plants. *Annu Rev Phytopathol.* 2006;44:135–62.
40. Li K, Wu G, Li M, Ma M, Du J, Sun M, et al. Transcriptome analysis of *Nicotiana benthamiana* infected by tobacco curly shoot virus. *Virology.* 2018;15(1):138. <https://doi.org/10.1186/s12985-018-1044-1>.
41. Bhat S, Folimonova SY, Cole AB, Ballard KD, Lei Z, Watson BS, et al. Influence of host chloroplast proteins on tobacco mosaic virus accumulation and intercellular movement. *Plant Physiol.* 2013;161(1):134–47. <https://doi.org/10.1104/pp.112.207860>.
42. Mochizuki T, Ogata Y, Hirata Y, Ohki ST. Quantitative transcriptional changes associated with chlorosis severity in mosaic leaves of tobacco plants infected with cucumber mosaic virus. *Mol Plant Pathol.* 2014;15(3):242–54. <https://doi.org/10.1111/mpp.12081>.
43. Xu Y, Zhou XP. Role of rice stripe virus NSvc4 in cell-to-cell movement and symptom development in *Nicotiana benthamiana*. *Front Plant Sci.* 2012;3:269.
44. Kong LF, Wu JX, Lu LN, Xu Y, Zhou XP. Interaction between Rice stripe virus disease-specific protein and host PsbP enhances virus symptoms. *Mol Plant.* 2014;7(4):691–708. <https://doi.org/10.1093/mp/sst158>.
45. Balasubramaniam M, Kim BS, Hutchens-Williams HM, Loesch-Fries LS. The photosystem II oxygen-evolving complex protein PsbP interacts with the coat protein of alfalfa mosaic virus and inhibits virus replication. *Mol Plant-Microbe Interact.* 2014;27(10):1107–18. <https://doi.org/10.1094/MPMI-02-14-0035-R>.
46. Bhattacharyya D, Chakraborty S. Chloroplast: the Trojan horse in plant-virus interaction. *Mol Plant Pathol.* 2017;19:504–18.
47. Ryals JA, Neuenschwander UH, Willits MG, Molina A, Steiner HY, Hunt, M.D. Systemic acquired resistance. *Plant Cell.* 1996;8(10):1809–19. <https://doi.org/10.2307/3870231>.
48. Von Broembsen SL, Deacon JW. Germination and further zoospore release from zoospore cysts of *Phytophthora parasitica*. *Mycol Res.* 1996;100(12):1498–150. [https://doi.org/10.1016/S0953-7562\(96\)80085-2](https://doi.org/10.1016/S0953-7562(96)80085-2).
49. Varet H, Brillatguéguen L, Coppée JY, Dillies MA. SARTools: a DESeq2- and EdgeR-based R pipeline for comprehensive differential analysis of RNA-Seq data. *PLoS One.* 2016;11(6):e0157022. <https://doi.org/10.1371/journal.pone.0157022>.
50. Colas V, Conrod S, Venard P, Keller H, Ricci P, Panabieres F. Elicitin genes expressed in vitro by certain tobacco isolates of *Phytophthora parasitica* are down regulated during compatible interactions. *Mol Plant-Microbe Interact.* 2001;14(3):326–35. <https://doi.org/10.1094/MPMI.2001.14.3.326>.
51. Yu G, Wang LG, Han Y, He QY. ClusterProfiler: an R package for comparing biological themes among gene clusters. *Omi AJ Integr Biol.* 2011;16:284–7.
52. Lu J, Du ZX, Kong J, Chen LN, Qiu YH, Li GF, et al. Transcriptome analysis of *Nicotiana tabacum* infected by cucumber mosaic virus during systemic symptom development. *PLoS One.* 2012;7(8):e43447. <https://doi.org/10.1371/journal.pone.0043447>.
53. Schmidt GW, Delaney SK. Stable internal reference genes for normalization of real-time RT-PCR in tobacco (*Nicotiana tabacum*) during development and abiotic stress. *Mol Gen Genomics.* 2010;283(3):233–41. <https://doi.org/10.1007/s00438-010-0511-1>.

Publisher's Note

Springer Nature remains neutral with regard to jurisdictional claims in published maps and institutional affiliations.

Ready to submit your research? Choose BMC and benefit from:

- fast, convenient online submission
- thorough peer review by experienced researchers in your field
- rapid publication on acceptance
- support for research data, including large and complex data types
- gold Open Access which fosters wider collaboration and increased citations
- maximum visibility for your research: over 100M website views per year

At BMC, research is always in progress.

Learn more biomedcentral.com/submissions

